Implantable Resonators – A Technique for Repeated Measurement of Oxygen at Multiple Deep Sites with In Vivo EPR

Hongbin Li, Huagang Hou, Artur Sucheta, Benjamin B. Williams, Jean P. Lariviere, Md. Nadeem Khan, Piotr N. Lesniewski, Bernard Gallez, and Harold M. Swartz

Abstract EPR oximetry using implantable resonators allows measurements at much deeper sites than are possible with surface resonators (> 80 vs. 10 mm) and achieves greater sensitivity at any depth. We report here the development of an improved technique that enables us to obtain the information from multiple sites and at a variety of depths. The measurements from the various sites are resolved using a simple magnetic field gradient. In the rat brain multi-probe implanted resonators measured pO_2 at several sites simultaneously for over 6 months under normoxic, hypoxic, and hyperoxic conditions. This technique also facilitates measurements in moving parts of the animal such as the heart, because the orientation of the paramagnetic material relative to the sensing loop is not altered by the motion. The measured response is fast, enabling measurements in real time of physiological and pathological changes such as experimental cardiac ischemia in the mouse heart. The technique also is quite useful for following changes in tumor pO_2, including applications with simultaneous measurements in tumors and adjacent normal tissues.

1 Introduction

EPR has been developed for over several decades and applied successfully for detecting and monitoring radical levels in chemical and biological materials [1–3]. L-band EPR, in particular, has been used for measuring and monitoring tissue pO_2 in rodents and in patients with subcutaneous tumors and skin cancer [4–5]. In spite of these successful applications, L-band EPR has some limitations such as being limited to measure at tissue depths of no more than 10 mm and considerable noise when measurements are made in organs that may move during the measurement, such as the beating heart. We have developed the

H.M. Swartz (✉)
EPR Center for Viable Systems, Department of Radiology, Dartmouth Medical School, 703, Vail, Hanover, NH 03755, USA
e-mail: harold.m.swartz@dartmouth.edu

E. Takahashi, D.F. Bruley (eds.), *Oxygen Transport to Tissue XXXI*, Advances in Experimental Medicine and Biology 662,
DOI 10.1007/978-1-4419-1241-1_38, © Springer Science+Business Media, LLC 2010

implantable resonators for EPR to overcome these limitations, to enhance detection, and to measure pO_2 in diverse tissues/organs. The techniques also have applicability for other types of measurements by EPR, including biophysical parameters, free radicals, redox state, and dosimetry.

2 Materials and Methods

The implantable resonator has two sets of loops, a larger loop on one end and one or more small loops on the other end. The large loop is used to couple inductively to the L-band EPR spectrometer. The small loop contains lithium phthalocyanine (LiPc) or other oxygen sensitive paramagnetic materials and is coated with a highly gas permeable, biocompatible material (in the studies we used Teflon) [6]. The small loops are implanted in the sites of interest.

All animal procedures were conducted in accordance with the NIH Guide and approved by the Institutional Animal Care and Use Committee of Dartmouth Medical School. The implantable resonators were placed surgically into regions based on the experimental designs. To measure pO_2 in the heart, a short single probe resonator was used. The large coupling loop was placed under the skin close to the chest, while the small tip was inserted into the myocardial muscle near the coronary artery of the mouse. After surgery, the animal was allowed to recover for a 2 days before the EPR measurements. To create temporary cardiac ischemia, a fine ligature was placed around the artery that could be tightened remotely to temporarily occlude the blood flow.

For brain pO_2, either a single or a multi-probe resonator was inserted into the targeted sites, while the large loop was placed on the scalp. Rats were allowed to recover for at least 1 day before hypoxic, normoxic, hyperoxic studies of brain tissue or measurements in tumors. The tumors were established by injection of a suspension of F98 glioma cells (500,000 cells/10μl, 7μl/site) intracranially at a depth of 5$\sim$6 mm from the skull into the vicinity of the sensing tip. To qualitatively assess the tumor growth and size, we used MRI to acquire images 1 day before and 19 days after the injection of F98 cells. MRI images were acquired on a 7T Varian console interfaced to a Magnex horizontal bore magnet using a birdcage coil in transmit/receive mode. T1-weighted images were acquired using a spin-echo sequence (repetition time, 0.7 s; excitation time, 9 ms; slice thickness, 1 mm; field of view, 4 $\times$ 4 cm; number of signal averages, 2; and matrix size, 128 $\times$ 128). The total data acquisition time was 3 min, 12 s for each image set.

EPR measurements were carried out using an L-band EPR spectrometer. Rats or mice were anesthetized with $\sim$2% isoflurane/air and were placed in the magnet with the resonator sensing tip in the center of the magnet. The loop of the external resonator was placed over the coupling loop of the implantable resonator. For multi-probe resonators, a single dimensional magnetic gradient was applied to separate the EPR signals from each probe. For normoxia, the

inhaled gas was 30% O_2; to induce mild hypoxia the gas was lowered to 15% O_2, and for hyperoxia we used carbogen (95% O_2/5% CO_2).

3 Results

Figure 1 shows the myocardial pO_2 during baseline and ischemic conditions. Under normoxia, the mouse had a very stable pO_2 of about 40 mmHg. With occlusion, the pO_2 immediately decreased to 15 mmHg. Upon reperfusion, the pO_2 increased but did not reach the baseline level. For repeated brain pO_2 measurements, a 3-probe resonator was placed into a rat brain with the following coordinates: Left, 3.5 mm with depth at 3.5, 1.5 mm with depth at 2.5 mm to the midline; right 1.5 mm with depth at 2.5 mm to the midline. The pO_2 measurement was started the second day after the resonator implantation and continued for up to 180 days, Fig. 2. In the first several days, tissue pO_2 showed

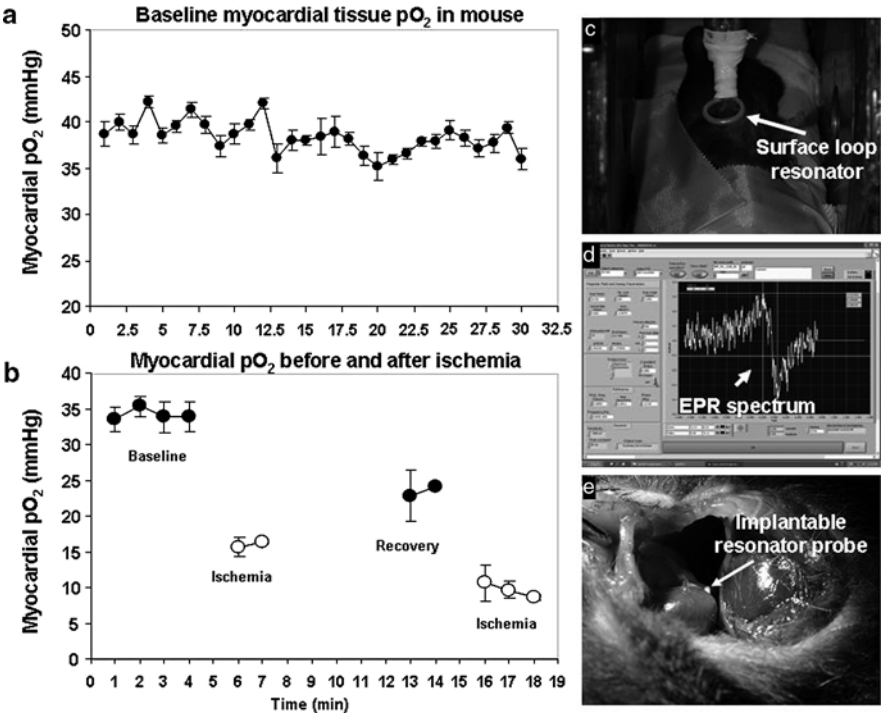

Fig. 1 Measurement of myocardial pO_2 using a short single probe resonator. **a**: baseline pO_2 of a mouse heart. **b**: pO_2 under several different conditions: baseline, ischemia and reperfusion. **c**: positioning of the external resonator over the large loop of the implantable resonator that was under the skin. **d**: a typical EPR spectrum (baseline pO_2). **e**: location of the resonator probe

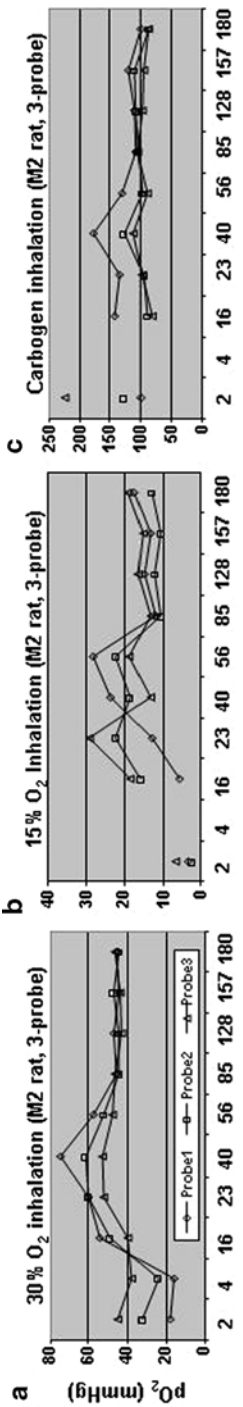

Fig. 2 Repeated, long term pO_2 measurements with a 3-probe resonator implanted in a rat brain. The measurements were started the second day after implantation and continued for up to 180 days. **a**: 30% O_2 for baseline, **b**: 15% O_2 for hypoxia and **c**: carbogen for hyperoxia

a large variation, which is likely due to the trauma associated with the insertion of the probes.

After 2 weeks, the tissue pO_2 stabilized and could be measured with a good signal to noise ratio in all measurements. The tissue pO_2 of a rat breathing 30% O_2 was 45 mmHg (Fig. 2a). Under 15% O_2, the rat had a pO_2 of 15 mmHg (Fig. 2b). When the rats breathed carbogen, the pO_2 increased to around 100 mmHg, (Fig. 2c). Importantly, there was no large variation in brain tissue pO_2 while breathing 30% O_2 from day 56 to 180. These results demonstrate the ability of this technique to monitor brain tissue oxygenation in both normal and pathologic conditions for prolonged periods of time.

For measuring the brain pO_2 dynamic changes, we used a 4-probe resonator implanted as indicated in Fig. 3. When the oxygen concentration was changed from 30% to room air, the brain pO_2 decreased gradually and reached a stable level after 10 minutes. Although all four sites did not have exactly the same pO_2 values, the dynamic patterns were very similar. When the oxygen level was changed from room air to 15% O_2, the tissue pO_2 in all sites reduced to much lower values (17∼22 mmHg). During a carbogen challenge, the two lateral sites had a much larger pO_2 response, compared to the two medial sites.

We inserted one-probe implantable resonators into the rat brain, at a depth of 5∼6 mm from the brain surface, for monitoring the pO_2 during tumor growth. Figure 4a shows the MRI images of a sham injected rat 7 days before and 19 days after an equal volume of culture media injection. There was no obvious morphological change in the MRI images. The pO_2 stayed at a very similar level (40∼55 mmHg) across the measurements (Fig. 4b). The changes in the MRI for the rats with tumors are shown in Fig. 4a, the tumor grew around the resonator tip. There was a decrease of the pO_2 in the tumor sites; the pattern of the decrease differed in different rats and showed different pO_2 decline rates (Fig. 4b). On day 25 after cell inoculation, all rats received carbogen. The brains in the sham injected rats had a robust response to the carbogen while the tumors had almost no response.

4 Discussion

We have successfully used implantable resonators to measure tissue pO_2 in the heart and the brain under diverse conditions. The use of the implantable resonators in the beating heart enabled us to overcome the problems usually encountered when trying to make measurements of pO_2 in a moving organ. Previously, to measure myocardial pO_2, we had to carry out a large amount of data averaging to reduce the noise induced by the relative motion between the paramagnetic material and the probe. This precluded measuring dynamic changes such as those associated with the acute induction of ischemia. Using a single or multi-probe resonator for long-term brain pO_2 measurements confirmed the very stable pO_2 in the targeted sites, and we were able to measure this

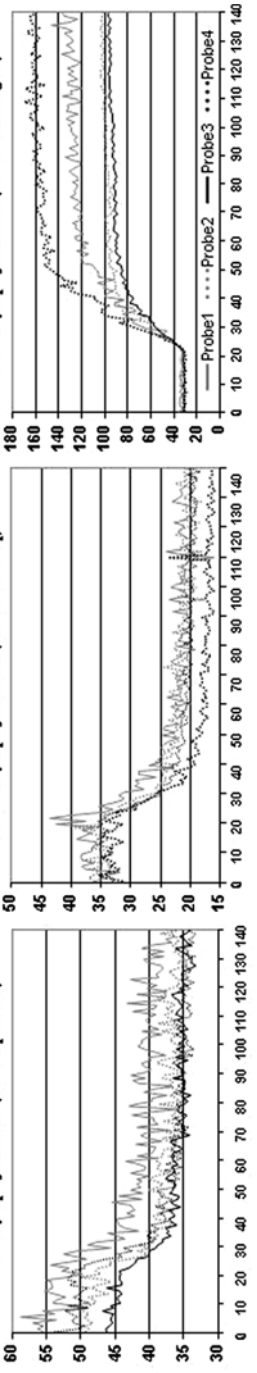

Fig. 3 A four-probe implantable resonator used to measure dynamic responses in the rat brain to changes in inhaled oxygen levels. The resonator was inserted at the following coordinates: AP, 0 mm; ML, 2.0 mm and 3.5 mm, DV, 5.5 mm. Oxygen was delivered through a nose cone to the rat. Plots from *left* to *right*: brain pO_2 during change from 30% O_2 to air, from air to 15% O_2, and from air to carbogen

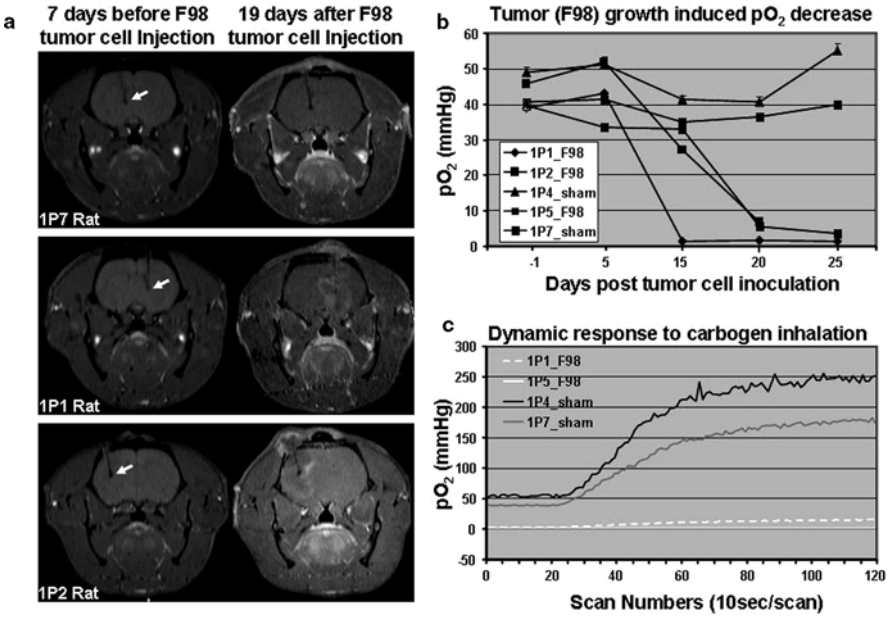

Fig. 4 pO_2 in rat F98 brain tumor measured with a single probe resonator. **a**: MRI images before and 19 days after F98 inoculation. *Arrows* indicate the probe locations in the brain. **b**: pO_2 measured the day before, 5, 15, 20 and 25 days after F98 inoculation in 3 rats with tumors and 2 sham rats. **c**: Carbogen challenge at day 25 after baseline pO_2

for days and months. Such measurements would be very difficult to do with polarographic electrodes or the OxyLite system.

Another very important advantage of this technique is the feasibility of carrying out oximetry at any depth. This extends the advantages of EPR oximetry to almost any site where the resonator can be implanted. The implantable resonators, once inserted, allow repeated pO_2 measurements with excellent time resolution and can be repeated across days or weeks.

Acknowledgments This work was supported by NIH grant PO1EB2180 and a Dartmouth NCCC Prouty Pilot Grant, and used the facilities of the EPR Center for Viable Systems (P41EB002032).

References

1. Swartz, H.M. and T. Walczak (1998) Developing in vivo EPR oximetry for clinical use. Adv Exp Med Biol 454:243–252.
2. Swartz, H.M. and B.A. Reichling (1978) The safety of X-ray examination of radioisotope scan. JAMA 239:2031–2032.

3. Hou, H., et al. (2007) The effect of oxygen therapy on brain damage and cerebral pO_2 in transient focal cerebral ischemia in the rat. Physiol Meas 28:963–976.
4. Som, S., et al. (2008) EPR oximetry in three spatial dimensions using sparse spin distribution. J Magn Reson 193(2):210–217.
5. Matsumoto, S., et al. (2008) Low-field paramagnetic resonance imaging of tumor oxygenation and glycolytic activity in mice. J Clin Invest 118:1965–1973.
6. Dinguizli, M., et al. (2006) Development and evaluation of biocompatible films of polytetrafluoroethylene polymers holding lithium phthalocyanine crystals for their use in EPR oximetry. Biosens Bioelectron 21:1015–1022.